Cheetah: A New Paradigm for Battery-free Wearable Devices

Vivian Dsouza*
Delft University of Technology
Delft, Netherlands
v.k.p.dsouza@tudelft.nl

Przemysł aw Paweł czak
Delft University of Technology
Delft, Netherlands
p.pawelczak@tudelft.nl

Alessandro Montanari
Nokia Bell Labs
Cambridge, United Kingdom
alessandro.montanari@nokia-bell-labs.com

Ashok Samraj Thangarajan
Nokia Bell Labs
Cambridge, United Kingdom
ashok.thangarajan@nokia-bell-labs.com

Abstract

Despite decades of research on battery-free systems, their adoption in everyday electronics remains limited. Interactive Internet of Things devices such as wearables, personal trackers, and health monitors are increasingly widespread, yet almost all depend on batteries that are environmentally harmful, slow to charge, and have limited lifespans. Existing battery-free devices have seen use only in niche applications with minimal user interaction, primarily due to slow energy harvesting, frequent power interruptions, and restricted sensing capabilities under tight energy constraints. To address these limitations, we present Cheetah, a battery-free architecture that charges rapidly and reliably from ubiquitous wireless chargers, reduces power consumption, and enhances usability. We implement and evaluate Cheetah architecture as a smartwatch and a wearable patch, capable of operating for a full day after only six seconds of charging. Our results demonstrate that battery-free design can move beyond niche deployments to become a practical and sustainable alternative for mainstream interactive electronics.

CCS Concepts

• **Computer systems organization** → **Embedded systems**; • **Hardware** → *Emerging architectures*; • **Human-centered computing** → *Ubiquitous and mobile computing design and evaluation methods.*

Keywords

Battery-free, Sustainability, Wearables, Ultra-fast Charging

ACM Reference Format:
Vivian Dsouza, Przemysł aw Paweł czak, Alessandro Montanari, and Ashok Samraj Thangarajan. 2026. Cheetah: A New Paradigm for Battery-free Wearable Devices. In *ACM/IEEE International Conference on Embedded Artificial Intelligence and Sensing Systems (SenSys '26), May 11–14, 2026, Saint Malo, France.* ACM, New York, NY, USA, 14 pages. https://doi.org/10.1145/3774906.3802775

*Work done by the author during his internship at Nokia Bell Labs, Cambridge, UK.

SenSys '26, Saint Malo, France

ACM ISBN 979-8-4007-2309-4/26/05
https://doi.org/10.1145/3774906.3802775

Figure 1: Demonstration of a user charging a Cheetah-enabled battery-free smartwatch within seconds via a smartphone using Qi wireless power transfer system.

1 Introduction

Battery-free systems have been extensively researched in the past years [4], yet they have hardly been used in day-to-day activities. To address this limited battery-free system adoption, in this work we present a simple but impactful idea—power battery-free devices in just a few seconds, and use them for the whole day or longer. Further, along with charging the device, the user automatically performs setup, synchronize the time and extract the data. This device could be a wearable such as a smartwatch, a health monitoring patch, or any other similar device, and it would charge reliably and quickly using a smartphone or any other wireless charger.

Not only does this approach reduce the number of batteries being used, it reduces the number of devices we require to charge for extended time. Instead of every individual having to charge multiple devices, (for example, their smartphone, laptop, watch, earbuds) end users would only charge a few of these larger battery-based devices, and use them in turn to charge smaller devices which remain battery-free.

1.1 Rapidly-charging Battery-free System

To achieve a truly ubiquitous battery-free deployment, we introduce Cheetah—a battery-free system architecture that charges a large supercapacitor rapidly with high power delivery from easily available wireless chargers based on Qi Wireless Power Consortium inductive charging (Qi) [8], as seen in Fig. 1. It communicates with a smartphone over Near Field Communication (NFC), and introduces dedicated enhancements that reduce system power consumption.

Cheetah can be used to either reduce the charging times of existing battery-systems, or increase the size of their storage capacitors to allow for longer lifetimes. It can also be used to convert existing battery-based devices to battery-free. Our contributions are:

(1) **Design Framework for Battery-free Systems:** Cheetah introduces a systematic design framework that explores the design space, trade-offs, and implementation considerations of battery-free devices. It captures key decisions spanning energy storage, ultra-low power communication, wake-up strategies, and user-perceived responsiveness, providing a foundation for developers to reason about design choices when building real-world battery-free applications.
(2) **Efficient Hardware and Software Co-Design:** We present the hardware architecture and software Application Programming Interfaces (APIs) that together enable an ultra-efficient energy harvesting and communication front-end. Through tight hardware–software co-design, Cheetah achieves seamless energy capture, rapid charge cycles, and efficient and responsive interaction, offering a developer-friendly interface for building fully battery-free, smartphone-connected systems.
(3) **Open Reference Platform:** We extensively evaluate Cheetah's several hardware and software sub-systems, and further demonstrate its drop-in integration with consumer electronics devices. The results show that Cheetah can operate in real-world conditions with minimal impact on functionality or user experience. To accelerate future research and adoption, we release all hardware and firmware as an open reference platform for the battery-free computing community [20].

1.2 Paper Structure

The remainder of this paper is structured as follows. Section 2 motivates the need for this approach and the gap that Cheetah addresses, and Section 3 highlights the state of the art. Section 4 outlines the system design and core principles behind Cheetah, followed by Section 5, which details our reference implementation. Section 6 presents a comprehensive evaluation of Cheetah's components and demonstrates a real-world device built using this architecture. We also examine how Cheetah can be integrated into commercial systems without compromising capability. Section 7 reflects on key design trade-offs and limitations, and Section 8 summarises the contributions and outlines future directions.

2 Motivation for Better Battery-free Devices

Energy harvesting systems aim to enable self-sustaining sensing by capturing ambient energy from sources such as light, vibration, thermal gradients, or radio frequency signals [4]. Two primary architectural paradigms exist: (i) intermittent systems [22] and (ii) energy-neutral systems [18]. *Intermittent systems* operate opportunistically, powering on when sufficient energy is available and check-pointing state to non-volatile memory before power loss. This architecture ensures forward progress in sensing and computation under extreme energy constraints. However, its inherently discontinuous operation limits responsiveness and usability in user-facing or time-sensitive applications, where latency, continuous feedback, or human interaction are essential.

In contrast, *energy-neutral systems* maintain continuous operation by carefully balancing harvested and consumed energy through adaptive duty-cycling, energy prediction, and dynamic performance scaling. They are better suited for continuous or interactive workloads, such as physiological monitoring or communication tasks, though their design complexity and dependency on predictable harvesting conditions restrict broader applicability.

Despite notable advances, fundamental problems for both intermittent and energy-neural systems, such as delivering quality of service under stochastic energy availability remains a challenge. In this paper, we ask the following question.

> Can energy-harvesting systems move beyond niche applications to deliver seamless, interactive performance suitable for real-world, user-facing applications?

Answering this question demands a fundamental rethinking of how energy is accumulated, managed, and expended, coupled with deep system-level optimisation. First, we discuss the limitations of existing systems.

***Limitation 1*—Issues with battery-powered devices:** The number of battery-powered devices used in everyday life continues to grow rapidly, as more and more devices become smart and interconnected. Alarmingly, an estimated 78 million batteries are discarded every day [1], and this number continues to grow. This trend is not sustainable, as batteries are severely polluting.

First, the extraction of minerals used in battery production (such as lithium) is a highly carbon-emitting process [24]. Furthermore, batteries have a limited number of charge–discharge cycles, requiring replacement every few years. Improper disposal further exacerbates the problem, as toxic elements from used batteries pollute the soil and water. In 2024, an estimated 10 billion battery replacements were made, with only about 5% being properly recycled [4], and the remainder accumulating in landfills and contributing to toxic electronic waste.

Beyond environmental concerns, the widespread use of batteries in household devices poses serious safety risks. Button cell batteries, in particular, have been linked to severe injuries and even fatalities in children [2, 29]. The number of pediatric battery related incidents has doubled over the last decade [7], underscoring the unintended consequences of the growing reliance on battery powered devices. These escalating challenges, spanning environmental degradation, health hazards, and long-term sustainability have prompted a critical re-evaluation of the battery-centric trajectory of the Internet of Things (IoT).

***Limitation 2*—Low adoption of existing battery-free devices:** Battery-free devices have long been positioned as a sustainable alternative to conventional battery-powered systems. These devices operate by harvesting energy from ambient sources—such as light, motion, or Radio Frequency (RF)—and storing it in capacitors or supercapacitors, which replace traditional batteries as the energy buffer. Their operation model is typically minimalist: remain dormant for long periods and opportunistically wake to perform brief, simple tasks when enough energy is available or at pre-defined intervals. Over the past two decades, research has demonstrated the feasibility of battery-free operation across a range of platforms,

including sensing nodes [3, 5, 15, 17, 31], smartwatches [10], gaming consoles [9], and even smartphones [26]. However, despite these technical successes, battery-free systems have failed to gain mainstream adoption, remaining confined to specialised domains—typically scenarios where battery replacement is impractical or maintenance-free operation is critical [3]. This lack of broader adoption stems from fundamental limitations: *severely constrained energy availability*, which drastically limits active task execution; *high latency and unreliability* from intermittent operation; and *significant development complexity*, as applications must be carefully tailored to cope with unpredictable energy budgets.

The early development of battery-operated devices such as wearables and mobile phones were fundamentally shaped by aggressive innovations in power management. Semiconductor manufacturers prioritised performance-per-watt, leading to the emergence of highly integrated, ultra-low-power System on Chips (SoCs). This, in turn, enabled the proliferation of wearables and a surrounding ecosystem comprising standardised battery chemistries, charging protocols (e.g., Qi, USB-C PD), and tightly coupled energy management stacks. In contrast, battery-free systems have not undergone a comparable systems level transformation. Despite over a decade of research into energy harvesting and battery-free platforms, these systems remain largely restricted to specialized applications where battery replacement is infeasible.

To summarize, in our view, the main barriers to the adoption of battery-free devices are the following factors:

(1) **Long charging times:** Existing battery-free devices take long to charge even when harvesting energy from externally powered sources.
(2) **Inconsistent power sources:** When relying on ambient energy sources such as sunlight, vibrations, or radio waves, charging can be unreliable. Devices may frequently discharge, and replenishing energy becomes difficult, particularly when the energy source is unavailable.
(3) **Reduced performance:** Many battery-free devices must operate at lower sampling rates or have shorter operational lifetimes due to the limited energy stored in capacitors.
(4) **Difficulty recovering from power failures:** These devices often face challenges in resynchronizing with time or recovering data after a power interruption.

Further, we believe that the main barriers to the adoption is not solely due to hardware limitations, but to an entrenched perception that battery-free devices are inherently impractical, slow to recharge, disruptive to use, and incapable of meeting real-time or interactive application demands. Overcoming this perception gap requires rethinking battery-free design around user-centric metrics, not just energy budgets.

To this end, we propose a new direction that advances battery-free systems toward real-world usability along three key dimensions: (i) ultra-fast energy replenishment using short, high-rate charging bursts; (ii) integration with ubiquitous infrastructure (e.g., consumer-grade charging points and RF interfaces); and (iii) interaction models with negligible friction, comparable to contactless payment systems. By reframing energy delivery and system responsiveness around convenience and integration, not just energy scarcity, we unlock a new design space for battery-free devices that are practical, deployable, and ready for everyday use.

3 Related Work

Battery-free devices have been explored across a wide range of applications, particularly in remote or inaccessible deployments where replacing batteries is impractical [4]. Research on battery-free interactive devices, where users can conveniently charge, access, and exchange data has been ongoing for over two decades. A summary of representative systems is provided in Table 1.

In this work, we focus on data-collecting battery-free devices designed for close-proximity use (that is, where close contact between a sensor and an interrogator such as a smartphone is required). These systems can be broadly categorized based on their energy-harvesting method, as described below.

(1) **NFC-based energy harvesting:** Several systems, such as *Densor* [13], *Biopulse* [23] and *NFC-WISP* [32], utilize NFC to both charge and communicate with a smartphone. These sensor platforms can use harvested energy to continuously monitor and collect user data such as health parameters, and share it through the same NFC interface. However, harvesting energy over NFC with these devices yields long charging times ranging from thirty seconds [13] to six minutes [23]. The power delivery of energy harvested via NFC is approximately 15 mW [32], which is significantly lower than the 1 W power delivery of the Qi standard proposed in this work.
(2) **Passive wearable devices powered by dedicated sources:** Recent work, e.g., *EverRing* [11], has demonstrated on-body wearables that harvest RF energy transmitted from nearby devices—in case of EverRing: a Virtual Reality (VR) headsets. These wearables operate passively and can be easily adapted to an actively-powered configuration using our proposed architecture, enabling faster energy replenishment and improved responsiveness.
(3) **Ambient energy harvesting from light or radio sources:** Other interactive systems, including the *FreeBie* smartwatch [10], *battery-free Gameboy* [9], and *Eyetracker* [19], harvest energy from ambient sources such as sunlight or radio signals. While sustainable, these sources are often unreliable and lead to frequent power interruptions, making the devices difficult to use consistently. Our proposed architecture can complement such systems by maintaining their original harvesting mechanisms while enhancing reliability and providing a more seamless user experience.

4 Cheetah System Architecture

We begin by outlining the core design principles underpinning Cheetah, followed by a detailed description of the hardware architecture and software framework that together form the complete Cheetah reference platform.

4.1 Cheetah Design Principles

For a new technology to be truly adopted, it must blend seamlessly with what people already understand, trust, and use daily [30]. The design of Cheetah adopts this principle: rather than introducing yet-another unfamiliar system, it re-imagines a technology that

Table 1: Related battery-free systems with a focus on energy storage and power delivery.

Study	Type	Energy (mJ)	Charge time (s)	Power (mW)	Energy source
NFC-Wisp [32]	Perishables monitoring	4.70	—	14.80†	NFC—Smartphone
Nicotine Sensor [21]	Vaping monitoring	Passive device only/No storage		2.00‡	NFC—Smartphone
AlterWear [12]	Wearable display	Passive device only/No storage		16.20◇	NFC—Smartphone
picoRing [25], EverRing [11]	Ring	Passive device only/No storage		3.50*	Induction, Radio
Densor [13]	Aligners	68.75	20	3.43	NFC—Smartphone
BioPulse [23]	Chest patch	5875.00	360	16.31	NFC—Smartphone
FreeBie [10]	Smartwatch	50.70	25	2.03	(Sun)light
Eye tracker [19]	Smartglasses	2327.60	—	0.80★	(Sun)light
CapBand [27]	Wristband	357.43	—	23.10⊕	Radio or Light
Cheetah (*This work*)	Patch, watch	5875.00	3.8	1546.05	Qi + NFC

Color scheme: As reported : The power delivery of charging is as stated in the research article. Calculated : The power delivery is calculated based on a full charge in the specified time period.

Notes: (values presented are best-case situation taken from the relevant article. Energy is calculated assuming a fully charged storage capacitor) † Article states 4 mA at 3.7 V. ‡ Taken from [21] Figure 4(a). ◇ Indicates power consumption in place of power delivery. * As reported in [11]. ★ Taken from [19] Figure 13(a). ⊕ Taken from [27, Section 9.4].

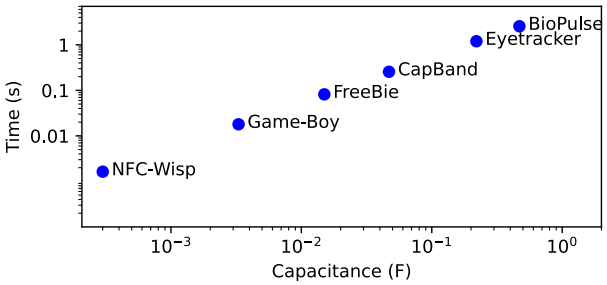

Figure 2: Theoretical time taken to charge the storage capacitors used in related work using wireless charging, assuming ideal power transfer of 1 W to 3.3 V. For this illustration, we use a conservative 1 W in the place of the potential 15 W of the Qi2 standard [8] to compensate for potential inefficiencies.

has seen limited acceptance, resolving its key limitations through a simple yet elegant redesign. By embedding this solution within an already ubiquitous and socially accepted platform, Cheetah leverages familiarity to overcome barriers to adoption. In the sections that follow, we outline the design principles that enable this seamless integration.

4.1.1 Fast charging. Fast, reliable, and user-friendly energy replenishment is fundamental to overcoming one of the greatest limitations of battery-free devices: charging latency. Unlike electrochemical batteries, which inherently require prolonged charging cycles, capacitors can absorb nearly all incoming power instantaneously, making rapid recharging achievable. As a result, the effective charging time is dictated not by the storage element itself, but by the power delivery capability of the energy source.

Because Cheetah targets close-proximity, user-interactive devices, we focus on charging methods that combine high power density with everyday accessibility. A straightforward approach is wired charging via Universal Serial Bus (USB) Power Delivery (PD) 3.0, capable of delivering up to 100 W [28]. While this ensures extremely fast and reliable charging, it introduces practical limitations: (i) as shown in Fig. 2, at such high input power, most capacitors reach full charge within seconds—making user interaction, rather than energy transfer, the dominant source of latency; and (ii) for on-body or sealed wearables, physical connectors compromise both aesthetics and reliability, making frequent plugging and unplugging impractical.

A more seamless alternative is wireless charging, now ubiquitous in consumer environments such as cars, furniture, and public spaces. Importantly, modern smartphones increasingly support reverse wireless charging, allowing them to not only charge themselves but also act as chargers for nearby devices. This capability transforms the smartphone into a portable, user-friendly power hub—a critical step toward truly interactive, battery-free operation. Motivated by these trends, Cheetah adopts a Qi-compatible wireless receiver, leveraging its ubiquity, safety, and effortless usability to enable instant, connector-free charging directly from the user's smartphone.

4.1.2 Synchronisation and Efficient Data Retrieval. Interactive wearable systems must stay synchronised with absolute time and support reliable data exchange for metrics such as step count, temperature, or heart rate. Battery-free devices, however, experience frequent power interruptions, requiring periodic resynchronisation and data offload to a smartphone. Existing systems typically use NFC for this purpose as seen in Table 1.

Interestingly, the Qi wireless charging standard, while primarily intended for power transfer, also supports bidirectional communication between the transmitter and receiver using frequency shift keying (FSK) and amplitude modulation (AM). Although this enables custom data transfer, its use in practice is constrained by: (i) limited smartphone support, as Android and iOS expose no developer APIs for Qi data exchange; (ii) low data rates compared to NFC; and (iii) lack of accessible non-volatile memory in commercial Qi front-ends. A comparison is shown in Table 2.

To harness the advantages of both, Cheetah employs a dual front-end architecture supporting Qi for high-power charging and NFC for synchronisation and data exchange. In use, the user rapidly

Table 2: Comparison between Qi and NFC standard for use with everyday battery-free devices.

	Power	Data rate	Compatibility*	NVM
Qi	15 W	2 kbps	Low	No
NFC	0.2 W	26 kbps	High	Yes

Color scheme: Indicates a desirable feature; NVM: Non Volatile Memory; *: ability to support a certain standard by a typical smartphone.

charges the device via Qi, then performs data retrieval and setup through NFC, all using a standard smartphone. Although Qi delivers up to 75 times more power, NFC provides sufficient energy to power the system transiently. The design should allow data transfer over NFC while being entirely powered by NFC without drawing from the main storage capacitor.

4.1.3 Hierarchical Energy Buffering and Precision Power Management. The most straightforward way to build a battery-free system is to simply replace the battery with a suitably sized capacitor. However, this naïve substitution introduces significant challenges. The capacitor must not be charged beyond the module's maximum operating voltage, and any attempt to regulate its output inevitably adds conversion losses—particularly during low-power sleep phases, when regulator quiescent currents can dominate total consumption. These trade-offs make it difficult to design a single, efficient power delivery path that performs well across all operating modes.

To address this, Cheetah introduces a new power management paradigm termed ***hierarchical buffering***. In this architecture, multiple energy buffers operate cooperatively, each optimized for a specific power regime. During active operation, the capacitor voltage is regulated to maintain the regulator's peak efficiency region, ensuring stable system performance. In contrast, during low-power or sleep states, the regulator is completely bypassed, and the system is powered by an alternate buffer that directly supplies the essential subsystems. This strategy enables autonomous switching between voltage domains, maintaining appropriate supply rails while drastically reducing power losses across modes.

Complementing this architecture, Cheetah employs ***precision sleep management*** to further extend runtime without sacrificing functionality. During idle periods, high-consumption components such as the Microcontroller Unit (MCU), sensors, and radios are completely powered down, with only the power management subsystem maintaining critical tasks like timekeeping and voltage monitoring. Where necessary, selected peripherals—such as low-power Inertial Measurement Units (IMUs)—can remain active in autonomous mode, continuing background operations even while the rest of the system is asleep. The system's software stack dynamically configures and powers these peripherals, ensuring that energy is allocated only where needed.

Together, *hierarchical buffering* and *precision sleep management* enable Cheetah to operate efficiently across dynamic power conditions, sustaining long energy-neutral operation on harvested energy.

4.1.4 Designing for Ultra-Low-Power and Energy-Neutral Sustainability. Achieving a truly battery-free system requires not only innovative power management strategies but also meticulous component selection to sustain reliable operation under extreme energy constraints. Every component from the storage capacitor to the MCU and communication interface contributes to the overall power budget and determines the practical usability of the platform.

Energy storage selection plays a pivotal role. The capacitor must be able to absorb harvested energy efficiently without introducing excessive Equivalent Series Resistance (ESR). Our measurements show that capacitors that higher ESR leads to longer charging times, drastically degrading the responsiveness and user experience of the device. Moreover, the trade-off between form factor and ESR cannot be ignored: in our observation, compact capacitors often employ dielectric materials with inherently higher ESR, thereby constraining charging efficiency and the achievable duty cycle.

Equally critical is minimising the sleep current, as the system spends the majority of its lifetime in quiescent states. The ability to retain context, periodically wake up, and control peripheral subsystems during these ultra-low-power intervals is essential for autonomous operation. Hence, the selection of components such as regulators, supervisors, and MCUs must strike a careful balance between functionality, wake-up flexibility, and low standby consumption.

Ultimately, the success of an energy-neutral platform hinges on these microscopic design choices, where even a few nanoamperes of leakage or a few ohms of ESR can be the determining factor between a responsive, perpetual system and one that fails to sustain itself on the harvested energy.

4.2 Cheetah Hardware Architecture

The hardware architecture of Cheetah is divided into three subsystems: (i) energy harvesting front-end and primary energy storage, (ii) power regulation and secondary energy buffer, and (iii) power management and time keeping. Furthermore, the design consists of an ultra-low power processor to run the Cheetah software stack. Fig. 3 shows the hardware architecture of Cheetah.

4.2.1 Energy Harvesting Front-end and Primary Energy Buffer. As described in Section 4.1.1 and Section 4.1.2, Cheetah integrates a Qi front end for rapid energy replenishment and an NFC front end for efficient data exchange. The system's default startup mode is Qi charging, ensuring that even when completely energy-depleted, it can first harvest sufficient power to boot and initialise communication. Once the Qi controller, or the measured capacitor voltage, indicates that charging is complete, the Cheetah stack switches to NFC mode to check for pending messages and perform data synchronization.

During NFC communication, the energy harvested directly from the NFC field is sufficient to power the entire logic subsystem. A smart power-routing switch disconnects the main energy buffer during this phase, allowing the device to operate solely from NFC power. This enables data retrieval "for free," preserving stored energy for sensing and computation. The software stack and smartphone application coordinate these transitions transparently, ensuring smooth handover between Qi charging and NFC communication without user intervention.

Together, these mechanisms make Cheetah function as a truly seamless, **tap-and-go system**—combining the instant convenience

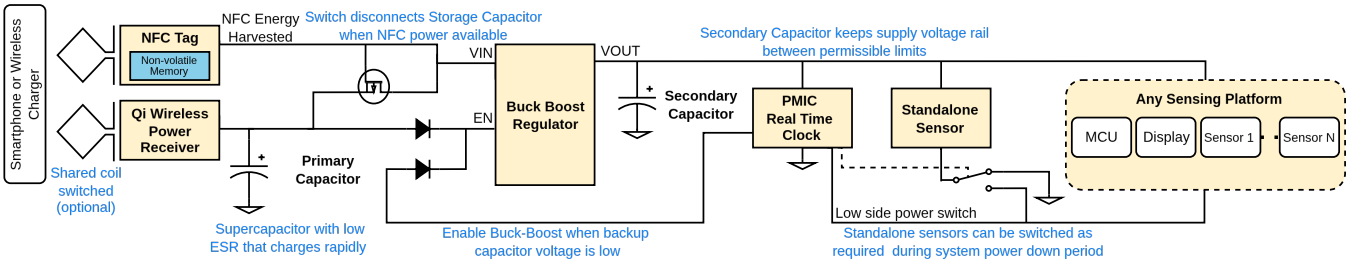

Figure 3: Cheetah system architecture showing the interaction between different components.

of wireless charging with the intuitive familiarity of NFC-based interaction.

4.2.2 Optimizing for Form-Factor Constraints. For applications with stringent space constraints, Cheetah adopts a shared-coil architecture that allows both the Qi and NFC to operate through a single antenna. In this design, an antenna coil of suitable inductance is alternately connected to either front end via a high-power single-pole double-throw (SPDT) switch. Individual matching networks are placed after the switch to ensure optimal tuning for each interface at its respective operating frequency. The MCU dynamically controls the switch, seamlessly selecting between Qi charging and NFC communication modes. To guarantee a reliable startup, the control line is pulled down by default, ensuring the system always initialises in the intended mode (e.g., Qi charging) even before firmware activation. The implementation is shown in Fig. 5.

While this approach introduces minor insertion loss and imperfect isolation, necessitating current limiting to protect the NFC front end, it offers a compact solution where physical space precludes the use of separate coils. The result is a space-efficient, dual-function interface that preserves full system capability.

4.2.3 Power Regulation and Secondary Energy Buffer. A critical challenge in battery-free design is deriving a stable and efficient supply rail from a charged storage capacitor. Most prior systems adopt one of the approaches illustrated in Fig. 4. In the simplest configuration (Design Ⓐ), the system operates directly from the capacitor voltage, occasionally protected by a Zener diode or low drop-out regulator (LDO) [13]. While this approach is simple and efficient, the capacitor can charge only up to the system's maximum voltage V_s (typically 3.3 V) and discharge down to its minimum operating limit $V_{\min}$ (typically 1.8 V). Because stored energy scales quadratically with voltage ($E = \frac{1}{2}CV^2$), this narrow range severely limits usable energy.

Design Ⓑ addresses this by placing a buck–boost regulator between the harvester and the system, allowing the capacitor to discharge over a wider voltage range. However, maintaining a regulated rail requires the regulator to remain continuously active, consuming tens of microamperes of quiescent current and introducing constant energy loss. Design Ⓒ improves efficiency by activating the converter only during harvesting, but again limits the storage voltage to the system's operating range, reducing the effective energy capacity.

To overcome these trade-offs, Cheetah introduces Design Ⓓ: a *hierarchical buffering architecture*. A large main capacitor is charged to a higher voltage to maximise stored energy, while a smaller secondary capacitor maintains the system's regulated rail. When the secondary capacitor voltage drops below a threshold, the Power Management Integrated Circuit (PMIC) briefly enables the buck–boost converter to replenish it from the main reservoir. This on-demand regulation minimises converter idle losses while sustaining a stable, energy-neutral supply, combining the efficiency of direct operation with the flexibility of active regulation.

Table 3: Comparison of voltage regulation methods used in various existing battery-free systems as seen in Fig. 4.

Type	Studies	$V_{C_{\text{high}}}$	$V_{C_{\text{low}}}$	E_c	I_q
Ⓐ	[13, 32]	$V_{s_{\max}}$	$V_{s_{\min}}$	3.82 J	None
Ⓑ	[23]	$V_{h_{\max}}$	$V_{b_{\min}}$	10.88 J	$I_{q_{\text{bb}}}$
Ⓒ	[9, 10]	$V_{s_{\max}}$	$V_{s_{\min}}$	3.82 J	$I_{q_{\text{bb}}}^{\dagger}$
Ⓓ	This work	$V_{h_{\max}}$	$V_{b_{\min}}$	10.88 J	$I_{q_{\text{bb}}}\, t_{\text{on}} + I_{\text{sd}}\, t_{\text{off}}$

$V_{C_{\text{high}}}$, $V_{C_{\text{low}}}$: high and low voltage on the capacitor, respectively; E_c: usable energy on the capacitor assuming $C = 1$ F given by $\frac{1}{2}\, C \left(V_{C_{\text{high}}}^2 - V_{C_{\text{low}}}^2\right)$; I_q: quiescent current; maximum supply voltage $V_{s_{\max}} = 3.3$ V; minimum supply voltage $V_{s_{\min}} = 1.8$ V; maximum voltage from harvester $V_{h_{\max}} = 5.0$ V; minimum input voltage for buck-boost converter $V_{b_{\min}} = 1.8$ V; t_{on}, t_{of}: time the buck-boost is on and off, respectively; $I_{q_{\text{bb}}}$: buck-boost quiescent current when on; I_{sd}: buck-boost shut down current when off; †: only when harvesting.

A summary of these options is given in Table 3. We observe that the effectiveness of our solution depends on the shutdown current of the buck-boost converter and its operational time. These results are evaluated in Section 6.

4.2.4 Power Management and Time Keeping. For most battery-free systems, power conservation is paramount. In Cheetah, all high-consumption components, such as the microcontroller and display, are fully powered down during sleep, while the design includes a dedicated PMIC that sustains only the essential housekeeping tasks: timekeeping, voltage supervision, and state retention.

When the system is brought close to a Qi charger, either after the storage capacitor is fully depleted or during a regular charging cycle, the charging field itself triggers a system wake-up. This is implemented by OR'ing the enable line of the main system regulator with the Qi front-end output, ensuring that the system powers up as soon as wireless power is detected. Once active, the system can then perform power management decisions and determine the appropriate operational mode.

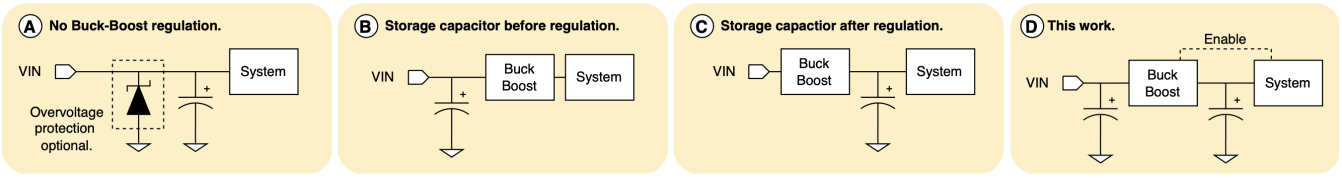

Figure 4: Common methods to achieve regulated supply voltage seen in battery-free system architectures. The advantages and drawbacks of each method are discussed in Section 4.2.3.

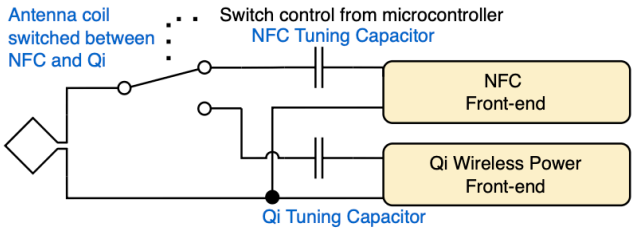

Figure 5: Shared antenna design for form factor-limited applications where two separate coils are not permissible.

To maintain responsiveness even in the absence of Qi power, Cheetah integrates multiple autonomous wake-up sources which are OR'ed to the main regulator enable, including: (i) a user button press, (ii) a timer-driven alarm interrupt, (iii) an NFC-triggered wake command, and (iv) a low-voltage event from the power monitor. Together, these mechanisms ensure that the system remains highly responsive and capable of initiating context-aware operations under varying energy conditions.

These mechanisms ensure that the system can transition instantly from deep sleep to active mode in response to user input, scheduled events, or energy conditions. Even in its lowest-power state, Cheetah remains context-aware and immediately accessible, balancing extreme energy efficiency with seamless user interaction.

4.2.5 Precision Power Management. Some peripherals can continue operating autonomously without continuous supervision from the microcontroller or other subsystems. For example, an IMU can perform step counting or motion detection in its own ultra-low-power mode. To exploit this capability, Cheetah enables selective activation of autonomous peripherals, allowing specific components to remain active even when the main system is powered down. This fine-grained control ensures that sensors operate only when functionally relevant, thereby minimising overall energy consumption.

To realise this functionality, Cheetah design uses a software-controlled SPDT low-side switch that dynamically toggles each sensor's ground connection. The switch connects the sensor either to the system's switched ground (disabling it) or to the common ground (keeping it active). During system shutdown, the microcontroller programs this control line to define which peripherals remain powered. Through this hardware–software co-design, Cheetah achieves precise control over peripheral activity, further extending operational lifetime and pushing the system toward true perpetual operation on harvested energy.

4.3 Cheetah Software Architecture

The Cheetah software architecture is designed to complement the hardware choices in Section 4.2, with a focus on efficiently managing the tight energy budget, ensuring robustness against power failures, enhancing usability, and minimising developer effort.

4.3.1 Setup and Synchronization. Cheetah operates in a cyclic sequence of *turn on* → *synchronise (if NFC detected)* → *sense* → *save* → *turn off*, designed to minimise energy consumption under intermittent power conditions. Since the MCU is fully powered down between cycles, each wake-up behaves as a cold start, effectively equivalent to a recovery from a power failure. This architecture naturally enforces atomic operation and state consistency, as every cycle begins from a deterministic initial state. Before power-down, all relevant sensor data and configuration parameters are securely stored in the non-volatile memory of the NFC tag.

Cheetah leverages the NFC interface as a unified channel for both data exchange and system control. When host NFC presence is detected (usually when the storage capacitor reaches full charge, and host switches from Qi to NFC), the device automatically issues a time-synchronisation request to the host. This can also be triggered programmatically via:

```
bool triggerTimeSynchronisation(uint8_t *timeStamp)
```

The host responds with the current Unix timestamp, which is written to the Cheetah's Real-Time Clock (RTC), ensuring precise timekeeping across operational cycles.

For temporal alignment, especially for user-visible timestamps and data correlation, the companion smartphone app periodically refreshes the time stored on the NFC tag. The *associated smartphone app* writes the current timestamp to a designated register, sets a synchronisation flag, and triggers an NFC interrupt to wake the MCU. Upon wake-up, the MCU reads the updated time, programs the RTC, and clears the flag, guaranteeing that all subsequent data samples remain accurately timestamped until the next recharge.

The NFC front-end can also assert an interrupt line, allowing the system to wake from deep sleep and respond to external commands on demand, offering a low-energy yet highly responsive interaction pathway between the device and the host.

4.3.2 Connectivity and Retrieving Data. For wearable devices such as smartwatches and health monitors, collecting and storing data such as heart rate and step count is essential. To make sensor configuration easily accessible, Cheetah allows users to write their preferred settings to the NFC tag. Upon each initialisation, the MCU retrieves these settings and applies them to the respective sensors

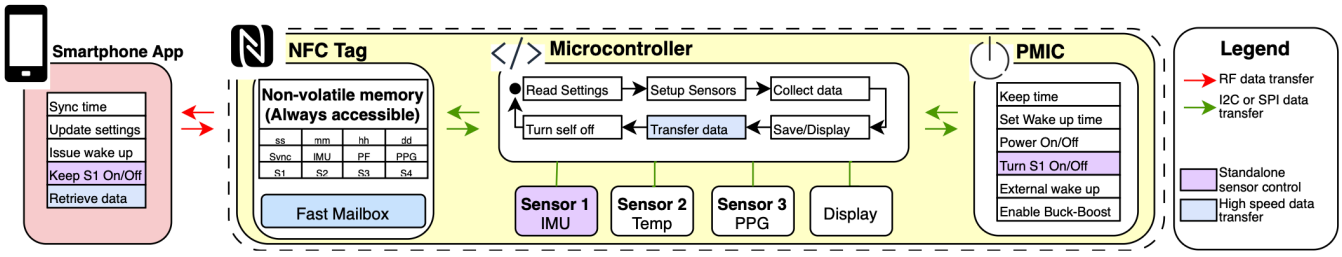

Figure 6: Software blocks of Cheetah. Notation: *Sx*: sensor *x* (or sensor *x* enable/disable flag); *issue wake up*: take action on the setting in the NFC tag; *sync*: time synchronization flag; *PF*: power failure flag; *ss, mm, hh, dd*: time/day flags; *IMU*: enable/disable IMU flag; *PPG*: enable/disable Photoplethysmography sensor flag.

via the Inter-Integrated Circuit (I^2C) interface. This approach ensures that all sensors are consistently configured according to user preferences, even after power loss.

The NFC interface provides a shared non-volatile memory space accessible to both the smartphone (via RF interface) and the MCU (via I^2C), enabling seamless bi-directional data exchange. For high-throughput transactions, Cheetah supports a mailbox-based communication mode, invoked using the following API call:

```
bool transferDataMBX(uint8_t *dataStream, uint16_t
    ↪ dataLength)
```

To retrieve the collected data, the user has two options: (i) store it in the Non Volatile Memory (NVM) of the NFC tag, or (ii) save it in the NVM of the MCU, or in an external NVM device integrated into the system.

Storing data on the NFC tag offers the advantage of immediate accessibility, as it can be directly read by a smartphone at any time. However, the memory capacity of the NFC tag is limited, and writing to its EEPROM is relatively slow and power-intensive. This method is therefore best suited for small amounts of data, such as summaries or configuration parameters.

For larger datasets, such as unprocessed sensor traces, the MCU can transfer data directly to the smartphone using a combination of I^2C and RF communication. This process, known as the *fast mailbox* mode, achieves significantly higher data rates as it draws power from the energy harvested through the NFC interface itself. Together, these methods balance accessibility and efficiency depending on the data volume.

4.3.3 Power Management and Failures. In addition, the user can decide whether the standalone sensors remain active or inactive in the next power cycle by setting the corresponding flag on the NFC tag. For example, a user may choose to enable specific sensors before an exercise session. Similarly, these decisions can also be made autonomously by logic implemented in the MCU, based on contextual factors such as time of day or previous activity. Once initialisation is complete, the MCU reads and, if required, processes the sensor data before storing or transmitting it. The application shall set the power configuration for peripherals using the following API call:

```
bool sensorLowPowerON(uint8_t sensorType, uint16_t
    ↪ sensorStatus)
```

In addition, when the system wakes up from sleep due to a low-voltage event in the secondary energy buffer, it transitions into a low-power charging mode. In this state, the system monitors the buffer voltage and allows the secondary capacitor to recharge safely. Once the charging process is complete, the system restores the previous configuration and returns to its ultra-low-power sleep state, ensuring stable operation without unnecessary energy expenditure. Under normal conditions, the secondary capacitor charges automatically during system operation. However, if the application needs to manually initiate charging or enter low-power charging mode, the following API can be used:

```
bool gotoChargerLowPowerMode(void);
```

For battery-free systems, handling power failures gracefully is essential to ensure a reliable and seamless user experience. Unlike battery-powered devices that maintain state across sessions, battery-free systems frequently lose power, making it crucial to preserve data integrity and recover predictably after each power cycle.

To ensure reliable operation, Cheetah always transfers configuration settings from non-volatile memory to the sensors at the start of each power cycle and saves all collected data before powering down. This atomic execution model guarantees that, although unexpected power losses may result in missing data, any stored data remains complete and accurately timestamped. Because the software architecture follows a sleep–wake cycle, it is inherently difficult to detect whether a power failure occurred between two cycles.

To address this challenge, Cheetah leverages the fact that the system time is synchronised each time it is recharged via the smartphone. Since a power failure results in the loss of time data, the system checks for a valid timestamp (for example, verifying that the recorded year is later than 2024). If a valid time is not found, the system assumes that charging and synchronisation are still in progress. As the charging process typically completes within a few seconds, the system uses the first valid timestamp as an indicator of a full charge and adjusts its energy budgeting accordingly.

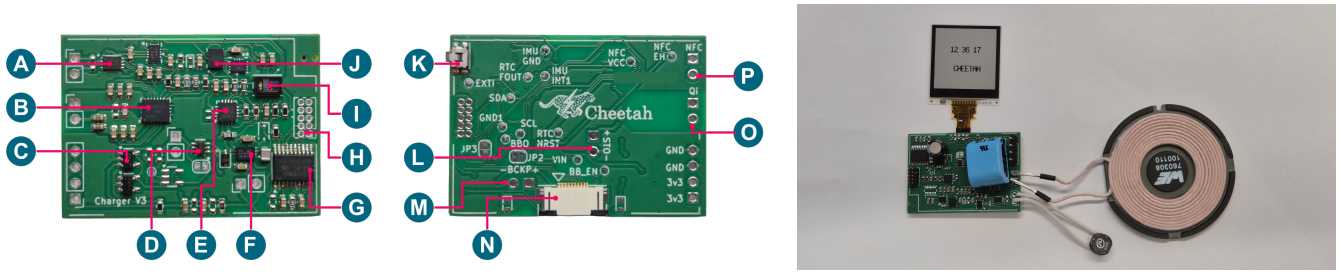

Figure 7: Left two images: Cheetah hardware after assembly (Front) A - ST25DV NFC Tag, B - BQ51013C Qi power receiver, C - MAX40200 ideal diode, D - SIP32432DR3 power switch, E - AM1805 RTC, F - ISL9122A buck-boost converter, G - STM32U031 MCU, H - debug port, I - MAXM86161 Photoplethysmography (PPG) sensor, J - LSM6DSOX IMU, (Back) K - pushbutton, L - primary capacitor connector, M - secondary capacitor connector, N - display connector, O - Qi antenna connector, P - NFC antenna connector. Right image: example assembled system.

5 Cheetah Architecture Implementation

5.1 Hardware Architecture Implementation

The hardware implementation adheres to the design principles outlined in Section 4.2, with a focus on achieving a compact form factor suitable for a smartwatch or a wearable patch.

5.1.1 Qi Charging. We employ the Texas Instruments BQ51013C to implement the Qi wireless power receiver front end, chosen for its compact package size and its ability to regulate output current. During capacitor charging, large inrush currents can occur, which may activate short-circuit protection mechanisms in other receiver designs. This issue is mitigated by configuring the charging current limit through an external resistor, as supported by the BQ51013C.

The antenna coil is tuned to resonate at 100 kHz. The series and parallel capacitances are selected according to the resonance condition $f = 1/(2\pi\sqrt{LC})$, where L is the coil inductance and C is the equivalent capacitance. To comply with the Qi standard, we ensure a quality factor $Q = (2\pi f L_s)/R > 77$, where L_s is the free space inductance and R is the Direct Current (DC) series resistance of the coil [16, Section 9.2.1.2.2]. The circuit is tuned for a coil inductance of 24 µH, and we evaluate multiple coil geometries with identical inductance but differing form factors and shielding configurations. For the optimized form factor for space constrained applications, we use the Analog Devices HMC784AMS8GE high power RF switch for its power capabilities and low insertion loss. We limit the current on the Qi wireless receiver when using this switch to prevent damage to the NFC tag from energy through imperfect isolation between channels.

5.1.2 NFC Communication. For the NFC communication interface, we use the STMicroelectronics ST25DV64K, selected for its compact package, energy-harvesting capability, and integrated NVM that can be accessed by both the smartphone and the MCU. The implementation of the NFC interface as a passive tag follows approaches similar to those described in prior works listed in Table 1. Additionally, we implement the *fast mailbox* mode to enable high-speed data transfer directly between the MCU and the smartphone.

To enable switching between the Qi and NFC paths, we employ the Vishay SIP32432DR3 power switch. A Nexperia 1PS76SB40 Schottky diode is used to prevent the input capacitor of the buck–boost converter from unintentionally keeping the power switch enabled; this ensures that the switch is activated only when energy is actively harvested from the NFC field.

The NFC tag serves dual roles: (i) it can act as a power source when the smartphone is present, and (ii) it can also require power during normal operation when data must be written to memory. To manage this bidirectional power relationship, we use a four-channel Texas Instruments TS3A44159 SPDT switch. Its low quiescent current and precise control allow the system to selectively disconnect the NFC tag's power and I^2C lines, preventing leakage currents and ensuring efficient operation during sensing cycles.

5.1.3 Power Management. For voltage regulation, we use the Renesas ISL9122AIRNZ buck-boost converter, chosen for its extremely low shutdown current of 8 nA. The converter's enable line is managed by the Abracon AB1805 RTC and power PMIC. This RTC is commonly employed in related works due to its ultra-low sleep current and ability to control power to external components. The ground connection of the standalone sensor is switched using a Texas Instruments TS3A44159 SPDT switch, also controlled by the AB1805.

To ensure that the buck-boost converter is enabled both during startup (when the backup capacitor has not yet charged) and when the backup capacitor voltage drops below its threshold, we employ two Analog Devices MAX40200 ideal diodes in an ORing configuration. One input of this OR connection is driven by the Qi power output, while the other is controlled by the AB1805 reset line, ensuring continuous and reliable system operation under all conditions.

5.1.4 Sensing System. Although the Cheetah architecture can be integrated with any system capable of communication over I^2C, in this work we implement a minimal sensing and display platform designed to function as a smartwatch or wearable patch. We employ the STMicroelectronics STM32U031F8 as the MCU due to its balance between low power consumption and sufficient performance, offering 64 kB of flash memory and 12 kB of RAM—adequate for a compact smart device. The STMicroelectronics LSM6DSOX IMU is used for its low-power operation and its ability to function as a standalone step-counting sensor.

Table 4: Cost breakdown of Cheetah hardware implementation with main components, excluding sensors and display.

	Part number	Cost (Euro)
NFC Tag	ST25DV04K-IER6T3	0.47
Qi Receiver	BQ51013CRHLR	1.52
Ideal diode	MAX40200AUK	0.88
PMIC/RTC	AM1805AQ	0.70
Buck-boost converter	ISL9122AIRNZ	1.14
MCU	STM32U031F8P6	0.90
Antenna	760308101312	6.60
PCB	Rigid FR4, 2–layer	2.26
Total		14.47

Note: Prices are per piece when buying a quantity of 1000.

We integrate the Analog Devices MAXM86161 PPG sensor to measure heart rate, as an example of physiological sensing system. An optional Sharp Microelectronics LS013B7DH03 memory Liquid Crystal Display (LCD) is included as a low-power display, connected via an flexible printed circuit connector (FPC) that allows easy removal when the display is not required. The MCU communicates with the NFC tag, RTC, buck–boost converter, IMU, and PPG sensor over I^2C, while the display is connected via Serial Peripheral Interface (SPI).

5.1.5 Fabrication. The circuit was fabricated on a rigid Printed Circuit Board (PCB) measuring 42 mm × 30 mm . Wire-to-board connectors were used to attach external antennas for both Qi and NFC, enabling evaluation of multiple antenna designs and configurations. The assembled hardware was enclosed in a 3D-printed case with a wrist strap (see again Fig. 1), forming a wearable smartwatch prototype. The cost of manufacturing Cheetah, excluding the sensors and display, is summarized in Table 4.

5.2 Software Architecture Implementation

The software implementation of Cheetah comprises two main components: (i) the development of the smartphone application, and (ii) the implementation of the MCU firmware. These two parts are designed to work in tandem—writing to the NFC memory via the smartphone directly triggers specific actions on the MCU, which executes the corresponding functions. This tight integration simplifies development and enhances usability.

The smartphone application was developed in Kotlin using Android Studio. It uses the `NfcV` class from the Android API to detect devices, and to send and receive custom commands and data over NFC. The application implements RF commands according to the STMicroelectronics ST25DV64KC specifications, enabling energy harvesting, interrupt generation to wake the system, and high-speed data retrieval via the fast mailbox mode. Although many recent smartphones support reverse Qi charging—marketed as Battery Share on the Google Pixel 9 and Wireless PowerShare on the Samsung S24—this functionality is not yet accessible through public software interfaces. As a result, users are required to manually enable and disable reverse charging. We anticipate that future software updates will provide programmatic control over this feature.

Table 5: Specification of supercapacitors used in the evaluation of fast charging.

	Part number	Size*	ESR (Ω)
C1	CE5R5105CF-ZJ	21.0 × 7.5	30.00
C2	CSP-6R0L105R-TW	16.0 × 8 × 19.5	0.24
C3	FG0H105ZF	16.5 × 19	65.00
C4	FS0H105ZF	28.5 × 14	7.00
C5	KR5R5H104R	11.5 × 5	75.00
C6	KVR5R0V105R	19.1 × 20.1	30.00

*: size denoted as diameter × height, or length × breadth × height, all in mm.

The MCU firmware was written in C using STM32CubeIDE, using 1.76 kB of Random Access Memory (RAM) and 15.86 kB of flash memory. The firmware provides a clear and modular API, allowing developers to extend or adapt Cheetah for a wide range of applications with minimal effort.

6 Cheetah Evaluation

6.1 Effect of ESR on Fast Charging

To assess the charging behavior of different supercapacitors using Qi wireless power transfer, we evaluated several 1 F capacitors listed in Table 5. These capacitors were empirically chosen with a reasonable form factor for a watch or patch, and with varying cost and ESR, in order to evaluate the effect of these parameters on the charging performance.

Measuring the charging process directly by monitoring the capacitor voltage during Qi charging can be misleading—especially for capacitors with high ESR. In such cases, the observed voltage reflects the open-circuit potential applied by the charger rather than the actual voltage across the capacitor. This can falsely suggest rapid charging, whereas the voltage in fact collapses immediately once the Qi power source is disconnected.

To address this issue, we instead characterized each capacitor by measuring the current drawn under a constant DC voltage. For this experiment, we used a Keithley 2450 SourceMeter, sourcing 5 V and recording the corresponding current. The resulting charge profiles for the different capacitors are presented in Fig. 8.

As shown in Fig. 8, the charging currents of the capacitors are initially high and gradually decrease as the capacitor charges. Capacitors with the lowest ESR charge the fastest, drawing a high initial current and reaching the end of the charging period more quickly. In contrast, capacitors with higher ESR are limited in the current they can draw initially, and continue to draw moderate current over an extended period. Therefore, for Qi charging, any supercapacitor can be used as long as its ESR does not become the limiting factor in the charging process.

6.2 Qi Charging Capacitors with Various Energy Sources

Next, we evaluate the time required to charge a supercapacitor using Cheetah. For this experiment, we use the implemented Cheetah hardware with the Wurth 760308101312 coil as the antenna. The supercapacitor selected is an Eaton PM-5R0V474-R with an ESR

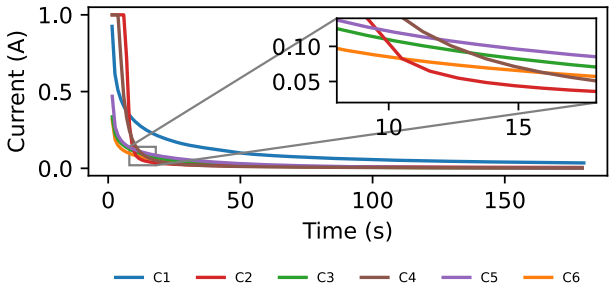

Figure 8: The charging current of various 1 F supercapacitors against time, with source voltage of 5 V and current limit of 1 A. Capacitors with lower ESR charge faster. In this graph, capacitor C2 charges the fastest.

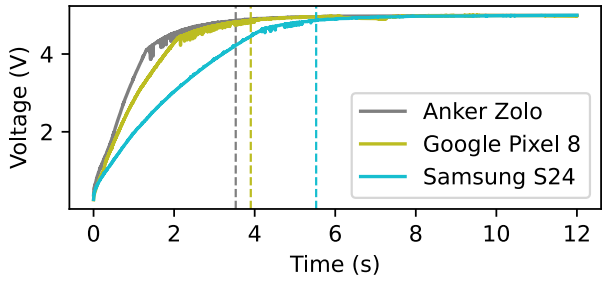

Figure 9: The time taken to charge a 0.47 F supercapacitor with energy harvested from Qi wireless charging. The vertical line, corresponding color-wise to each charging platform, indicates the time taken for the capacitor to reach 95 % of full charge.

of 0.42 Ω. This capacitor has a compact form factor suitable for a smartwatch or wearable patch, and its capacity matches that used in Biopulse [23], where it was charged via NFC in approximately 6 min. The voltage across the capacitor was measured using the Saleae Logic Pro 8 logic analyzer, and the traces are synchronized by starting when the voltage curve first crosses 0.2 V.

For the Qi wireless power source, we evaluate three devices: (i) an Anker Zolo wireless charger connected to a wall outlet, (ii) the Google Pixel 8 smartphone using *Battery Share*, and (iii) the Samsung Galaxy S24 with *Wireless PowerShare*. Using Cheetah, the capacitor is fully charged in under 6 s, as shown in Fig. 9, representing an approximately 60-fold improvement over NFC-based charging reported in related work.

6.3 Hierarchical Charging

To evaluate the operation of the hierarchical charging architecture, we charge Cheetah using Qi power and measure the voltages across both the primary and secondary capacitors using a Saleae Logic Pro 8 logic analyzer. The Eaton PM-5R0V474-R is used as the primary energy storage capacitor, while the Seiko CPH3225A serves as the secondary capacitor. The RTC is configured to raise an

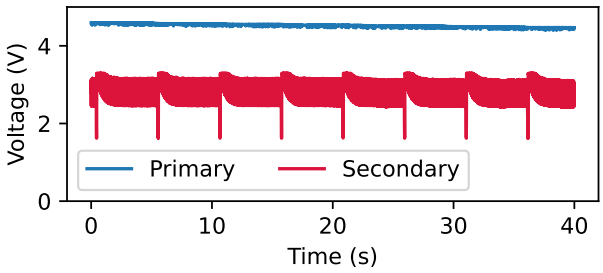

Figure 10: Charging of the secondary from the primary capacitor. Each time the voltage on the secondary capacitor falls below 2.5 V an interrupt is raised and the buck-boost is enabled to recharge it.

Table 6: Current consumption of the ISL9122A buck-boost used in hierarchical charging.

Mode	Specification (nA)	Measured (nA)	Time (ms)
Disabled	8	430	4475
Enabled	1300	1600	656

(1) **Specification:** typical values for current consumption as specified in the datasheet; **Measured:** actual current consumption measured by Keithley 2450 Source meter at no load condition.

interrupt when the voltage of the secondary capacitor drops below 2.5 V. As shown in Fig. 10, the secondary capacitor is periodically recharged from the primary capacitor in distinct cycles. When the system is powered down, the buck–boost converter is disabled to minimize power consumption. Once the system supply rail, maintained by the secondary capacitor, falls below the threshold voltage, the buck–boost converter is re-enabled and the cycle resumes. Each interrupt event triggers a system wake-up, during which an inrush current is drawn, causing a transient drop in the supply voltage rail. It should be noted that the measurement probes of the logic analyzer themselves draw approximately 0.5 µA, which slightly influences the observed results.

To quantify the power savings achieved by the proposed method, we compare it against a configuration in which the buck–boost converter remains continuously enabled. We measure both the quiescent and shutdown currents of the converter, as well as the duration spent in each mode during operation. The results, summarized in Table 6, indicate that for the selected capacitor configuration, our approach achieves a power reduction of 63.7%.

6.4 Capacitor to Capacitor charging efficiency

We also evaluate the efficiency of the capacitor-to-capacitor energy transfer using the buck-boost converter. The energy transfer efficiency η, i.e. the ratio of the total energy delivered to the secondary capacitor to the energy lost from the primary capacitor, is given as

$$\eta = \frac{N_{\text{cycles}} C_{\text{secondary}} \left(V_{\text{high}}^2 - V_{\text{low}}^2 \right)}{C_{\text{primary}} \left(V_{\text{start}}^2 - V_{\text{end}}^2 \right)}. \quad (1)$$

Table 7: Power consumption of Cheetah in various operation states.

State	Measured current	Power
Shutdown (*sd*), power off	28 nA	92.4 nW
Standalone (*sa*), only IMU on	8 µA	26.4 µW
Power on (*on*), awake	1.7 mA	5.61 mW

We observe the voltage across both the primary and secondary capacitors over $N_{\text{cycles}} = 3$ charge-discharge cycles, where the secondary capacitor is charged from $V_{\text{low}} = 2.5\,\text{V}$ to $V_{\text{high}} = 3.3\,\text{V}$. During this period, the voltage on the primary capacitor decreases from $V_{\text{start}} = 4.61\,\text{V}$ to $V_{\text{end}} = 4.556\,\text{V}$. We used $C_{\text{primary}} = 0.47\,\text{F}$ and $C_{\text{secondary}} = 0.011\,\text{F}$. The energy efficiency is 65.82%. Thus, although the available energy is reduced, the power consumption decreases even more to 36.3%. Consequently, the overall efficiency of this approach represents a 1.81-fold improvement compared to system with the buck–boost converter continuously on.

6.5 Power Consumption

To evaluate the power consumption we measure the current consumed using the Keithley 2450 source-meter when sourcing 3.3 V. The results are given in Table 7. The power off current is determined mainly by the RTC, the supply current of the switches to prevent leakage current, and pull-up resistors. When the IMU is kept on as a standalone sensor, the power consumption increases to enable continuous sensing. The power on current consists of the MCU running at 16 MHz, and all sensors on. Cheetah lifetime depends on the primary and secondary capacitors, and the usage profile.

To estimate L, the expected operational system lifetime, we model L as the ratio of the available stored energy to the average power consumption as

$$L = \eta \frac{\frac{1}{2} C_{\text{primary}} \left(V_{\text{high}}^2 - V_{\text{low}}^2 \right)}{V_{\text{system}} \left(\frac{I_{\text{sd}} T_{\text{sd}} + I_{\text{sa}} T_{\text{sa}} + I_{\text{on}} T_{\text{on}}}{T_{\text{total}}} \right)}, \tag{2}$$

where C_{primary} is the primary storage capacitance, V_{high} and V_{low} are the upper and lower operating voltages of the capacitor, respectively, V_{system} is the system supply voltage, I_{sd}, I_{sa}, and I_{on} are the shutdown, stand-alone sensor operation, and system on currents, respectively, T_{sd}, T_{sa}, and T_{on} are the durations for which the system remains in each state as listed in Table 7, T_{total} is the total duration of the operational cycle, and η is given in Eq. (1).

Using Eq. (2), we calculate the lifetime an example user profile. For instance, with 0.47 F capacitor, if the system was running with the IMU always on to perform step counting, and fully powered on for 10 s of each hour—the device stays powered for 22 h.

6.6 Form Factor

As the physical bulk of capacitors can also limit the adoption of battery-free systems, we examine the relationship between capacitor volume and performance. Having established that the charging time is proportional to the ESR in Section 6.1, we now analyze how ESR varies with the physical volume of the capacitor, as shown in Fig. 11. We observe a general inverse relationship—capacitors with larger volumes tend to exhibit lower ESR values and therefore charge more rapidly. However, several outliers exist that achieve relatively low ESR despite smaller form factors, making them particularly attractive for compact, battery-free designs.

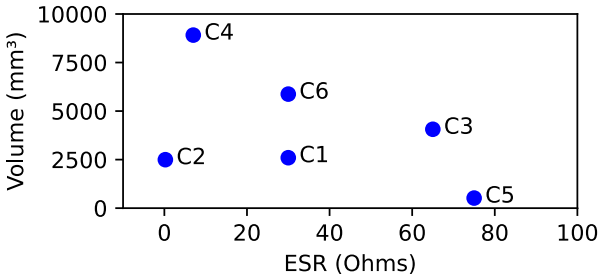

Figure 11: Relation between the ESR and physical volume of various 1 F supercapacitors listed in Table 5.

6.7 Application Examples

Beyond user-worn devices, Cheetah can also be applied to convert existing battery-powered systems into battery-free alternatives. By replacing conventional batteries with capacitors, these devices not only become more sustainable by reducing battery waste, but also benefit from the ability to recharge within seconds when they are needed. This approach is particularly well-suited for intermittently used devices such as weighing scales, remote controls, electronic toys, and other small household appliances.

As an example, we examine the feasibility of adapting commercial smart trackers, such as the Apple AirTag, into battery-free devices. To date, over 55 million AirTags have been sold [14], each powered by a coin cell battery that typically requires annual replacement. In its current design, the AirTag exhibits a sleep current of approximately 2.3 µA [6]. By leveraging the ultra-low power characteristics of Cheetah, the standby current during power-off can be reduced to the nanoampere range, extending the device's operational lifetime. Based on our calculations derived from the measured power consumption, as reported in [6], if the AirTag were redesigned to be battery-free using a 1 F capacitor with no other optimizations, it would achieve an operational duration of approximately 42 h on a single charge. The lifetime can be further increased by modifying the behavior of the smart tracker, such as when and how often it advertises over Bluetooth Low Energy (BLE). For example, if the BLE advertisements were once every 5 s, in the place of the presently used 2 s it would increase the lifetime to 4.4 days on a single charge. If such devices could be recharged wirelessly in the background,they could operate entirely battery-free, thereby eliminating the need for millions of batteries.

7 Discussion and Future Work

Power Limit. While the Qi standard supports power transfer levels of up to 15 W, in this work we limit the received power to 1.5 W. This choice reflects our observation that charging time is no longer the primary bottleneck at this scale. Increasing the storage

capacity by employing larger supercapacitors could further extend operational energy reserves, provided that the form factor permits.

Communication over Qi. In this work, we introduce a dual front-end architecture to ensure compatibility between power transfer and communication interfaces. However, in principle, data communication could be directly modulated onto the Qi charging waveform itself. Future devices may provide access to the Qi communication channel or dynamically reconfigure the antenna to operate at a different bandwidth after charging, thereby enabling higher data rates. Alternatively, synchronization could also be achieved over longer-range wireless links such as Bluetooth or cellular networks, if the system already includes such connectivity.

Comparison with Battery Powered Devices. While Cheetah offers better battery-free device operation, its performance still lags behind similar-sized battery powered devices. Unlike battery based systems that stay powered continuously, Cheetah requires duty-cycling to achieve similar lifetimes. Algorithms to control the duty-cycling to achieve battery-like performance are needed.

8 Conclusion

We propose Cheetah: a new architecture for battery-free devices equipped with an existing NFC interface. In this design, an additional wireless charging front end based on the Qi Wireless Power Consortium inductive charging (Qi) interface is integrated, enabling rapid recharging of a capacitor. This essentially simple system architecture offers a low-hanging fruit solution to a major challenge faced by battery-free devices: namely, the short operational time of (super-)capacitors, prolonged charging durations via the NFC interface, and the intermittent availability of harvested energy.

Acknowledgments

The authors thank the anonymous reviewers and the shepherd for their valuable feedback during the review process. The authors also thank Marc Van Den Broeck and Ananta Narayanan Balaji from Nokia Bell Labs for their valuable support and guidance.

References

[1] 2021. *78 Million Batteries will be Dumped Every Day by 2025.* https://www.imec-int.com/en/press/78-million-batteries-will-be-dumped-every-day-2025 Last accessed: 13 Nov. 2025.

[2] 2021. *Two-year-old's Button Battery Death Sparks Warning.* https://www.bbc.co.uk/news/uk-england-stoke-staffordshire-57553914 Last accessed: 13 Nov. 2025.

[3] Mikhail Afanasov, Naveed Anwar Bhatti, Dennis Campagna, Giacomo Caslini, Fabio Massimo Centonze, Koustabh Dolui, Andrea Maioli, Erica Barone, Muhammad Hamad Alizai, Junaid Haroon Siddiqui, and Luca Mottola. 2020. Battery-Less Zero-Maintenance Embedded Sensing at the MithræUm of Circus Maximus. In *Proc. SenSys.* ACM, Virtual Event, 368–381. https://doi.org/10.1145/3384419.3430722.

[4] Saad Ahmed, Bashima Islam, Kasım Sinan Yıldırım, Marco Zimmerling, Przemysław Pawełczak, Muhammad Hamad Alizai, Brandon Lucia, Luca Mottola, Jacob Sorber, and Josiah Hester. 2024. The Internet of Batteryless Things. *Commun. ACM* 67, 3 (March 2024), 64–73. https://doi.org/10.1145/3624718.

[5] Abu Bakar, Rishabh Goel, Jasper de Winkel, Jason Huang, Saad Ahmed, Bashima Islam, Przemysław Pawełczak, Kasım Sinan Yıldırım, and Josiah Hester. 2023. Protean: An Energy-Efficient and Heterogeneous Platform for Adaptive and Hardware-Accelerated Battery- Computing. In *Proc. SenSys* (Boston, MA, USA). ACM, 207–221. https://doi.org/10.1145/3560905.3568561.

[6] Adam Catley. 2022. *Apple AirTag Reverse Engineering.* https://adamcatley.com/AirTag.html Last accessed: 13 Nov. 2025.

[7] Mark D. Chandler, Khudeja Ilyas, Kris R. Jatana, Gary A. Smith, Lara B. McKenzie, and J. Morag MacKay. 2022. Pediatric Battery-Related Emergency Department Visits in the United States: 2010–2019. *Pediatrics* 150, 3 (2022). https://doi.org/10.1542/peds.2022-056709.

[8] Wireless Power Consortium. 2025. Wireless Power Consortium (Qi Standard). https://www.wirelesspowerconsortium.com/standards/qi-wireless-charging/ Last accessed: 14 Nov. 2025.

[9] Jasper de Winkel, Vito Kortbeek, Josiah Hester, and Przemysław Pawełczak. 2020. Battery-Free Game Boy. *Proc. ACM Interact. Mob. Wearable Ubiquitous Technol.* 4, 3 (Sept. 2020), 111:1–111:34. https://dl.acm.org/doi/abs/10.1145/3411839.

[10] Jasper de Winkel, Haozhe Tang, and Przemysław Pawełczak. 2022. Intermittently-powered Bluetooth that Works. In *Proc. MobiSys.* ACM, Portland, OR, USA, 287–301. https://doi.org/10.1145/3498361.3538934.

[11] Nathan DeVrio and Chris Harrison. 2025. EverRing: Powering Battery-Free, Highly-Capable Smart Rings with Headset RF Energy. In *Proc. ISWC.* ACM, Espoo, Finland, 68–75. https://doi.org/10.1145/3715071.3750420.

[12] Christine Dierk, Molly Jane Pearce Nicholas, and Eric Paulos. 2018. AlterWear: Battery-Free Wearable Displays for Opportunistic Interactions. In *Proc. CHI.* ACM, Montreal, QC, Canada, 220:1–220:11. https://doi.org/10.1145/3173574.3173794.

[13] Vivian Dsouza, Jeffrey Pronk, Christian Peppelman, Víctor Ignacio Madariaga, Tatiana Pereira-Cenci, Bas Loomans, and Przemysław Pawełczak. 2024. Densor: An Intraoral Battery-Free Sensing Platform. *Proc. ACM Interact. Mob. Wearable Ubiquitous Technol.* 8, 4 (May 2024), 191:1–191:30. https://doi.org/10.1145/3699746.

[14] Yahoo Finance. 2022. *Apple AirTags and Bluetooth Trackers Are Officially a Billion-Dollar Industry.* https://finance.yahoo.com/news/apple-airtags-bluetooth-trackers-officially-175911565.html Last accessed: 13 Nov. 2025.

[15] Josiah Hester and Jacob Sorber. 2017. Flicker: Rapid Prototyping for the Batteryless Internet-of-Things. In *Proc. SenSys* (Delft, The Netherlands). ACM, 19:1–19:13. https://doi.org/10.1145/3131672.3131674.

[16] Texas Instruments. 2025. BQ51013C: Highly Integrated Wireless Receiver Qi (WPC v1.3) Compliant Power Supply. https://www.ti.com/lit/ds/symlink/bq51013c.pdf Last accessed: 14 Nov. 2025.

[17] Neal Jackson, Joshua Adkins, and Prabal Dutta. 2019. Capacity Over Capacitance for Reliable Energy Harvesting Sensors. In *Proc. IPSN* (Montreal, Quebec, Canada). ACM, 193–204. https://doi.org/10.1145/3302506.3310400.

[18] Aman Kansal, Jason Hsu, Sadaf Zahedi, and Mani B. Srivastava. 2007. Power Management in Energy Harvesting Sensor Networks. *ACM Trans. Embed. Comput. Syst.* 6, 4 (Sept. 2007). https://doi.org/10.1145/1274858.1274870.

[19] Tianxing Li and Xia Zhou. 2018. Battery-Free Eye Tracker on Glasses. In *Proc. MobiCom.* ACM, New Delhi, India, 67–82. https://doi.org/10.1145/3241539.3241578.

[20] Nokia. 2026. Wearable Battery-free Frontend. https://github.com/nokia/Wearables-BatteryFree-Frontend Last accessed: 24 Mar. 2026.

[21] Md. Ataur Rahman, Le Cai, Sherif Abdulkader Tawfik, Stuart Tucker, Alex Burton, Ganganath Perera, Michelle J. S. Spencer, Sumeet Walia, Sharath Sriram, Philipp Gutruf, and Madhu Bhaskaran. 2022. Nicotine Sensors for Wearable Battery-Free Monitoring of Vaping. *ACS Sens.* 7, 1 (Dec. 2022), 82–88. https://doi.org/10.1021/acssensors.1c01633.

[22] Benjamin Ransford, Jacob Sorber, and Kevin Fu. 2011. Mementos: System Support for Long-running Computation on RFID-scale Devices. In *Proc. ASPLOS.* ACM, Newport Beach, CA, USA, 159–170. https://doi.org/10.1145/1950365.1950386.

[23] C Rajashekar Reddy, Vivian Dsouza, Ashok Samraj Thangarajan, Przemysław Pawełczak, Fahim Kawsar, and Alessandro Montanari. 2025. BioPulse: Towards Enabling Perpetual Vital Signs Monitoring using a Body Patch. In *Proc. HotMobile.* ACM, La Quinta, CA, USA, 103–108. https://doi.org/10.1145/3708468.3711891.

[24] Sebastian Schaal. 2025. How Much CO2 does Battery Production Really Emit? https://www.electrive.com/2025/08/17/how-much-co2-does-battery-production-really-emit/ Last accessed: 14 Nov. 2025.

[25] Ryo Takahashi, Eric Whitmire, Roger Boldu, Shiu Ng, Wolf Kienzle, and Hrvoje Benko. 2024. picoRing: Battery-free Rings for Subtle Thumb-to-index Input. In *Proc. UIST.* ACM, Pittsburgh, PA, USA, 13:1–13:11. https://doi.org/10.1145/3654777.3676365.

[26] Vamsi Talla, Bryce Kellogg, Shyamnath Gollakota, and Joshua R Smith. 2017. Battery-free Cellphone. *ACM Interact. Mob. Wearable Ubiquitous Technol.* 1, 2 (June 2017), 25:1–25:19. https://doi.org/10.1145/3090090.

[27] Hoang Truong, Shuo Zhang, Ufuk Muncuk, Phuc Nguyen, Nam Bui, Anh Nguyen, Qin Lv, Kaushik Chowdhury, Thang Dinh, and Tam Vu. 2018. CapBand: Battery-free Successive Capacitance Sensing Wristband for Hand Gesture Recognition. In *Proc. SenSys.* ACM, Shenzhen, China, 54–67. https://doi.org/10.1145/3274783.3274854.

[28] USB Implementers Forum, Inc. 2025. USB Charger (USB Power Delivery). https://www.usb.org/usb-charger-pd Last accessed: 14 Nov. 2025.

[29] Fergus Walsh. 2016. *Button Batteries pose 'deadly' Risk to Toddlers.* https://www.bbc.co.uk/news/health-37410343 Last accessed: 13 Nov. 2025.

[30] Mark Weiser. 1991. The Computer for the 21st Century. *Scientific American* 265, 3 (1991), 94–105. https://www.jstor.org/stable/24938718.

[31] Fan Yang, Ashok Samraj Thangarajan, Gowri Sankar Ramachandran, Bhaskar Krishnamachari, Wouter Joosen, Christophe Huygens, and Danny Hughes. 2019. Astar: Sustainable Battery Free Energy Harvesting for Heterogeneous Platforms and Dynamic Environments. In *Proc. EWSN.* ACM, 71–82. https://dl.acm.org/doi/10.5555/3324320.3324329.

[32] Yi Zhao, Joshua R. Smith, and Alanson Sample. 2015. NFC-WISP: A sensing and computationally enhanced near-field RFID platform. In *Proc. RFID.* IEEE, San

Diego, CA, USA, 174–181. https://doi.org/10.1109/RFID.2015.7113089.